2-1-2020

# Evidence of increased hypoxia signaling in fetal liver from maternal nutrient restriction in mice.

Bethany N Radford

Victor K M Han
victor.han@lhsc.on.ca

Pediatric RESEARCH

BASIC SCIENCE ARTICLE

# Evidence of increased hypoxia signaling in fetal liver from maternal nutrient restriction in mice

Bethany N. Radford[1,2] and Victor K. M. Han[1,2,3]

**BACKGROUND:** Intrauterine growth restriction (IUGR) is a pregnancy condition where fetal growth is reduced, and offspring from IUGR pregnancies are at increased risk for type II diabetes as adults. The liver is susceptible to fetal undernutrition experienced by IUGR infants and animal models of growth restriction. This study aimed to examine hepatic expression changes in a maternal nutrient restriction (MNR) mouse model of IUGR to understand fetal adaptations that influence adult metabolism.
**METHODS:** Liver samples of male offspring from MNR (70% of ad libitum starting at E6.5) or control pregnancies were obtained at E18.5 and differential expression was assessed by RNAseq and western blots.
**RESULTS:** Forty-nine differentially expressed (FDR < 0.1) transcripts were enriched in hypoxia-inducible pathways including Fkbp5 (1.6-fold change), Ccng2 (1.5-fold change), Pfkfb3 (1.5-fold change), Kdm3a (1.2-fold change), Btg2 (1.6-fold change), Vhl (1.3-fold change), and Hif-3a (1.3-fold change) (FDR < 0.1). Fkbp5, Pfkfb3, Kdm3a, and Hif-3a were confirmed by qPCR, but only HIF-2a (2.2-fold change, $p = 0.002$) and HIF-3a (1.3 $p = 0.03$) protein were significantly increased.
**CONCLUSION:** Although a moderate impact, these data support evidence of fetal adaptation to reduced nutrients by increased hypoxia signaling in the liver.

*Pediatric Research* (2020) 87:450–455; https://doi.org/10.1038/s41390-019-0447-z

## INTRODUCTION

Intrauterine growth restriction (IUGR) is a pregnancy condition where fetal growth is suboptimal, resulting in an infant born with a birth weight <10th percentile.[1] Individuals born from pregnancies complicated by IUGR are at increased risk for peri and postnatal complications and, as adults, are at increased risk for metabolic disorders.[2] Adverse intrauterine conditions may lead to adaptations to enhance fetal survival but contribute to aberrant metabolism as adults.[2]

Hypoxia-inducible factor (HIF) pathway is a cellular response to enhance survival in adverse conditions, such as hypoxia and nutritional stress. Under normal physiological conditions, the a subunit (HIF-1a, HIF-2a, HIF-3a) is posttranslationally hydroxylated and/or phosphorylated in the cytosol by regulators such as von Hippel–Lindau (VHL)/U3 ligase complex, factor inhibitor of hypoxia (FIH), and glycogen synthase kinase 3β (GSK-3β).[3–5] These posttranslational modifications promote proteasomal degradation.[3–5] During cellular stress, reduced hydroxylation and/or phosphorylation at stabilization sites inhibit recognition by the proteasome. Stabilization in the cytosol results in increased dimerization with the HIF-1β subunit. HIF dimers then translocate to the nucleus and transcriptionally regulate genes containing hypoxia-responsive elements (HREs).[5] HRE-containing genes are involved in metabolism, cell cycle regulation, and angiogenesis.[4,6]

Adaptations in HIF signaling in the placentas from growth-restricted pregnancies or kidney and liver of maternal nutrient restriction (MNR) IUGR animal models have been documented.[7,8] However, others fail to find differences in HIF signaling in these tissues.[9,10] Previously, we have shown that MNR results in male offspring with reduced fetal and adult liver size and increased hepatic insulin sensitivity in adulthood.[11] Here we aimed to investigate whether HIF signaling has a role in fetal liver adaptations. Our results suggest that MNR in mice induces hypoxia-inducible signaling in the fetal liver. Such adaptations to growth and metabolism in the developing liver may contribute to long-term metabolic impacts of IUGR.

## METHODS

### Animals

All animal procedures were approved by the Animal Use Subcommittee of the University Council on Animal Care at the University of Western Ontario and were described by Radford and Han, 2018.[11] Briefly, mice were housed in 12-h light and dark cycles. Virgin 8-week-old CD-1 females were bred, and the presence of a vaginal plug indicated E0.5. At E6.5, pregnant females received *ad libitum* standard chow (control, $N = 5$) or MNR ($N = 5$) (70% total calories) (#F0173, Bio-Serv, Flemington, NJ). At E18.5, dams were euthanized with $CO_2$ narcosis and pups with cervical dislocation. Right liver lobes were removed from each pup, snap frozen in liquid nitrogen, and stored at −80 °C. Male offspring from MNR have been reported to be more sensitive than females to the long-term changes in glucose metabolism,[12] and only metabolic changes in males have been investigated previously in this model.[11] Male fetuses were identified with SRY PCR (forward primer—TGGACTGGTGACAARGCTA, reverse primer—TGGAAGTACAGGTGTGCACTCT) and used for further analysis.

[1]Department of Biochemistry, Schulich School of Medicine & Dentistry, Western University, London, ON, Canada; [2]Children's Health Research Institute, London, ON, Canada and [3]Department of Pediatrics, Schulich School of Medicine & Dentistry, Western University, London, ON, Canada
Correspondence: Victor K. M. Han (Victor.Han@lhsc.on.ca)

Received: 19 December 2018 Revised: 19 April 2019 Accepted: 18 May 2019
Published online: 11 June 2019

RNA isolations
RNA for sequencing was isolated from ten control and ten MNR livers (two mice per litter). Additional RNA isolations from eight control and eight MNR littermates (one or two mice per litter) were used as a validation cohort for real-time PCR. Briefly, the frozen right liver lobe (30–50 mg for sequencing and 10–15 mg for real-time PCR) was pulverized with a Bessman Tissue Pulverizer (Spectrum Laboratories, Rancho Dominguez, CA), then homogenized with a Brinkman homogenizer Polytron® 3000 for 50 s in 1 mL or 500 µL of ice-cold TRIzol, respectively. RNA was collected from the homogenate with the PureLink Mini RNA Kit (Invitrogen, Carlsbad, CA) using the TRIzol Plus RNA Purification Kit protocol provided by the manufacturer. DNA was degraded with the on-column DNAse I treatment option in the provided protocol (Roche, DNAseI recombinant, RNAse-Free, Cat. No. 716728, Mannheim, Germany). RNA was eluted from the column with 25 µL of UltraPure™ DNase/RNase-Free Distilled Water (ThermoFisher Scientific, Cat. No. 10977015, Carlsbad, CA) after a 5-min on-column incubation. Samples were aliquoted into smaller volumes and stored at −80 °C until further studies.

RNA sequencing
RNA/library QC and RNA sequencing was run at McGill University and Genome Quebec Innovation Centre, Quebec, Canada. Libraries were generated with the NEBNext® Ultra™ Directional RNA Library Prep Kit for Illumina® (E7420S, New England BioLabs, MA, USA). Quality of RNA was verified on the Agilent Bioanalyzer (RIN > 7). Single-read 50 bp sequencing was obtained from a HiSeq 2500 with 17–31M reads per sample (average depth of 23M). Reads were aligned to the mm9 transcriptome[13] with Bowtie2[14] (90% alignment rate). Aligned and raw read counts are deposited in NCBI's Gene Expression Omnibus (GSE124006).[15]

Real-time PCR
cDNA was generated with the SuperScript™ IV First-Strand Synthesis System (Invitrogen, Vilnius, Lithuania) with 1 µg of RNA per reaction using the concentrations estimated by the Agilent Bioanalyzer. Taqman assays that covered multiple exons were purchased for select target genes including: Ccng2 (4448892, Mm00432394_m1), Btg2 (4453320, Mm00476162_m1), Kdm3a (4448892, Mm01182127_m1), Fkbp5 (4448892, Mm00487406_m1), Pfkbp3 (4448892, Mm00504650_m1), Hif-3a (Mm00469375_m1), Vhl (Mm00494137_m1), Hif-1a (Mm00468869_m1), and Hif-2a (Mm01236112_m1); and endogenous controls Gapdh (4331182, Mm99999915_g1) and beta actin (4331182, Mm01205647_g1) (Invitrogen, Vilnius, Lithuania). Reactions were run with diluted cDNA (1:5) and the TaqMan™ Fast Advanced Master Mix (Invitrogen, Vilnius, Lithuania) on the ViiA™ 7 (Applied Biosystems, Carlsbad, CA) fast 384-well block setting according to the manufacturer's protocol. Fold change was calculated using the delta delta CT method (ddCT) and the average CT value of actin and GAPDH as the reference.

Protein isolations
In all, 10–15 mg of tissue was homogenized with 1 mL of ice-cold 1× Cell Lysis buffer (9803 S) from Cell Signaling (Danvers, MA) with protease inhibitor cocktail 1, 2, and 3 (P1860, P5726, and P0044, Sigma-Aldrich, St. Louis, MO) for 40 s with a Brinkman homogenizer Polytron® 3000. Lysates were sonicated (F550 Sonic Dismemberator, Fisher Scientific, Markham, ON) and then shaken at 4 °C for 2 h. Cellular debris was removed from lysates by spinning at 12,000 × *g* for 10 min and the supernatant was collected for analysis. Protein concentrations were calculated with the Bio-Rad Protein Assay (Cat #500–0006, Bio-Rad Laboratories Inc., Des Plaines, IL) according to the manufacturer's protocol.

Western blotting
Fifty µg of protein for HIF-2a blots and 25 µg for all other blots were loaded and run on an 8% polyacrylamide gel. Protein was transferred to a polyvinylidene difluoride membrane with the Transblot Turbo™ (Bio-Rad Laboratories Inc., Des Plaines, IL). Membranes were dipped in methanol and then blocked for an hour at room temperature in 5% milk in TBST (TBS+0.1% tween). After rinsing 3 times (5 min each) in TBST, primary antibodies were incubated in 5% bovine serum albumin in TBST overnight (Table 1). Blots were rinsed 3 times (5 min each) and incubated with secondary antibodies in 5% milk in TBST for 1 h at room temperature (Table 1). Blots were imaged with the Clarity™ Western ECL Substrate (1705061, Bio-Rad Laboratories Inc., Des Plaines, IL), and band intensities were quantified using the Imagelab software® version 5.1 BETA (Bio-Rad Laboratories Inc., Des Plaines, IL). As a loading control, all blots were rinsed 3 times with TBST (5 min each), stripped with 0.5 M sodium hydroxide for 15 min, and re-probed for actin according to the protocol above. Each target band was normalized to the respective actin and the control group was used to calculate relative fold changes. KDM3a was not assessed via western blot because we were not able to find an effective antibody for the mouse fetal liver samples. All blots were run in triplicate.

Statistical analysis
Samples that contributed more variation than expected to each group were removed as outliers as described by Gierliński et al. with the mean+2 times the interquartile range as the threshold.[16] Differential expression was detected with a false discovery rate (FDR) <0.1 with consistency in ≥2 tools (EdgeR,[16] DESeq2,[17] and ALDex2[18]) using the default settings in R (version 3.4.3). Optimal number of clusters were generated with the gap statistic with the Cluster library (version 2.0.6) and principle component analysis (PCA) plots were plotted with ggplot2 (version 2.2.1) and ggrepel (version 0.8.0) in the R console (version 3.3.2 and 3.4.3). Gene ontology (GO) pathway enrichment was done on the GO Tool (Panther)[19]; and KEGG and NCI pathway enrichments were run on enrichR.[20] For quantitative PCR (qPCR) and western blots, unpaired *t* tests were used to compare delta CT values or band intensities on Graphpad Prism (version 5.2).

**Table 1.** Western blot antibodies

| | Target | Company | Source | Cat. no. | Dilution |
|---|---|---|---|---|---|
| Primary | HIF-2a | Santa Cruz Biotechnology Inc. (Dallas, TX, USA) | Mouse | sc-13596 | 1:250 |
| | HIF-3a | Santa Cruz Biotechnology Inc. (Dallas, TX, USA) | Mouse | sc-390933 | 1:200 |
| | FKBP5 | Santa Cruz Biotechnology Inc. (Dallas, TX, USA) | Mouse | sc-271547 | 1:200 |
| | PFKFB3 | Cell Signaling (Danvers, MA, USA) | Rabbit | 13123S | 1:1000 |
| | Actin | ThermoFisher Scientific (Fremont, CA) | Mouse | MS-1295-PCL | 1:2000 |
| Secondary | Mouse IgG | Bio-Rad Laboratories Inc. (Hercules, CA) | — | 170–6515 | 1:10,000 |
| | Rabbit IgG | Bio-Rad Laboratories Inc. (Hercules, CA) | — | 170–6515 | 1:10,000 |

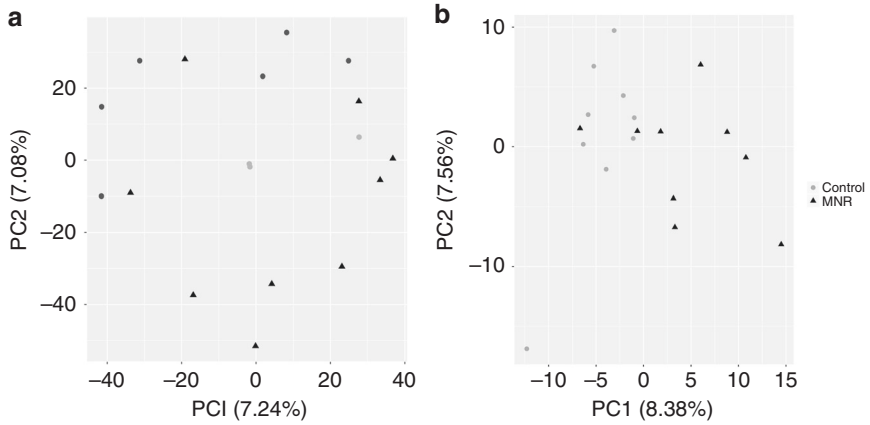


**Fig. 1** Principle component analysis of the top 500 variable genes. Data were transformed with the centered-log ratio (**a**) and regularized-log ratio (**b**). Control $N = 9$ and maternal nutrient restriction $N = 9$, 1–2 pups/litter

## RESULTS

RNA sequencing data were assessed for sample outliers and gene distributions among remaining samples.[16] One control and one MNR sample contributed more variance to their respective maternal nutrient groups than other samples within the group and were removed from further analysis (Supplementary Fig. S1). With remaining samples, two distributions of genes were formed along PC1 (Supplementary Fig. S2). The second distribution contained genes enriched in GO pathways in neural and epithelial cell development (Supplementary Table S1), since hepatocyte and hematopoietic populations are of primary interest in this study this second distribution of genes was removed from the analysis.

Overall gene expression was explored with PCA plots and cluster analysis. The optimal number of clusters with the gap statistic of the centered-log ratio and regularized-log ratio transformed data was 1. However, *k*-means clusters with $k = 2$ resulted in clusters separating based on counts per sample (Supplementary Fig. S1a and Supplementary Table S2). The PCA plot of the top 500 variable genes from the centered-log ratio (Fig. 1a) did not result in separation of samples based on maternal nutrition. Although the PCA of the top 500 variable genes of the regularized-log ratio transformed data indicate moderate separation of maternal nutrition along PC1, the first component only explains 8% of the total variance (Fig. 1b). These plots suggest that overall gene expression was similar between the control and MNR fetal livers.

Despite similar overall expression, 49 protein-coding genes were differentially expressed in MNR fetal livers relative to controls using a FDR cut-off of <0.1 and consistency of two or more tools (Supplementary Table S3). GO enrichment indicated negative regulation of transcription from RNA polymerase II promoter in response to hypoxia as the top pathway when ranked according to fold enrichment (Cited2 and Vhl) (Fig. 2a). Hypoxia signaling was also the top pathway enrichment according to combined scores with KEGG (Fig. 2b) and NCI (Fig. 2c). Additional genes included in these enrichments are Pfkfb3 and Hif-3a. Investigation into gene functions of differentially expressed genes indicate further involvement in cellular response to hypoxia (Fig. 3).

Genes involved in hypoxic regulation of metabolism, cell cycle regulation, and chronic hypoxia were selected to be validated by qPCR in a separate validation cohort (Fig. 4). Pfkfb3 transcript was increased 1.8-fold ($p = 0.002$) in MNR relative to controls, similar to the fold change in the RNAseq data of 1.5 (FDR = $1.2 \times 10–6$). Fkbp5 and Kdm3a transcripts were also confirmed to be increased by 1.3- and 1.5-fold ($p = 0.03$ and 0.02) and similar to sequencing fold changes of 1.6 and 1.2, respectively (FDR = 0.006 and 0.04). Lastly, Hif-3a was significantly higher by 1.4-fold in the MNR livers in the validation cohort ($p = 0.01$), similar to the 1.3-fold increased initial MNR cohort (FDR = 0.009). Although not significant, Ccng2, which was 1.5-fold higher in the RNAseq data (FDR = 0.0001), was relatively higher in the MNR fetal livers by 1.4-fold ($p = 0.05$). Btg2 and Vhl were not significantly different in the validation cohort ($p = 0.1$ and 0.7). Both Btg2 and Ccng2 had high variation among MNR offspring and a small fold change relative to controls (<2). Larger sample sizes could be required to confirm changes in Btg2 and Ccng2 transcripts. Hif-1a and Hif-2a transcripts were not significantly different in the initial MNR cohort, but Hif-1a was 1.3-fold decreased in the validation MNR group relative to controls ($p = 0.01$).

Protein levels for genes differentially expressed in the validation cohort were determined by western blots (Fig. 5). Since the HIF alpha subunits can be regulated posttranscriptionally in response to cellular stress, the protein levels were also measured. HIF-1a was not detected in the fetal liver (Supplementary Fig. 3) but HIF-2a was increased 2.2-fold in MNR fetuses ($p = 0.002$). HIF-3a was also increased by 1.3-fold ($p = 0.03$) in MNR relative to controls (Fig. 5a, b). FKBP5 (1.6-fold change, $p = 0.09$) and PFKFB3 (1.3-fold change, $p = 0.5$) protein levels were not significantly different between the maternal nutrient groups (Fig. 5c, d).

## DISCUSSION

Fetal growth restriction leads to increased risk for perinatal complication and changes to adult glucose metabolism in adults.[1,2] Currently, no treatments are available to address these perinatal and long-term concerns in IUGR infants. Identification of pathways altered in response to restricted growth *in utero* in metabolically important tissues, such as the liver, provide potential targets for therapeutic intervention. HIF signaling is a pathway that has gained recent attention in growth-restricted offspring; however, evidence of HIF induction has been conflicting and tissue specific.[8–10] The approach taken in this study was unbiased, investigating relative transcript levels of all protein-coding genes, and supports the concept that HIF signaling is induced in the MNR fetal liver of male offspring from moderate MNR. This underlines the importance of further studies to determine how hepatic HIF signaling influences fetal survival and long-term glucose metabolism in response to fetal undernutrition.

HIF-2a protein was increased in MNR offspring, but HIF-1a was not detected. Normal development in cells, such as endothelial cells, involve a switch from HIF-1a to HIF-2a as the primary HRE transcriptional regulator,[21] similar to the transition observed with chronic hypoxia in cancer cells.[22,23] In these tissues, this switch is thought to occur in part because oxygen tension increases as organ perfusion during development becomes more efficient. FIH and prolyl hydroxylases less efficiently hydroxylate HIF-2a allowing

**a**

| | Go pathway | Fold enrichment | FDR |
|---|---|---|---|
| 1 | Negative regulation of transcription from RNA polymerase II promoter in response to hypoxia (GO:0061428) | >100 | 3.78E–02 |
| 2 | Negative regulation of transcription from RNA polymerase II promoter in response to stress (GO:009701) | >100 | 1.73E–02 |
| 3 | Regulation of DNA-templated transcription in response to stress (GO:0043620) | 32.45 | 2.03E–02 |
| 4 | Skeletal muscle cell differentiation (GO:0035914) | 30.29 | 2.04E–02 |
| 5 | Muscle tissue development (GO:0060537) | 8.29 | 4.07E–02 |
| 6 | Blood vessel morphogenesis (GO:0048514) | 7.74 | 2.49E–02 |
| 7 | Blood vessel development (GO:0001568) | 6.2 | 5.01E–02 |
| 8 | Response to hormone (GO:0009725) | 6.11 | 2.87E–02 |
| 9 | Cellular response to stress (GO:0033554) | 4.03 | 2.52E–02 |
| 10 | Positive regulation of RNA metabolic process (GO:0051254) | 4.02 | 1.70E–02 |


**Fig. 2** Top 10 gene ontologies (**a**), KEGG (**b**), and NCI:Nature (**c**) gene pathway enrichments with protein-coding genes differentially expressed between control and maternal nutrient restriction **b**, **c** Significant pathways are in red and the bar size represents the combines score

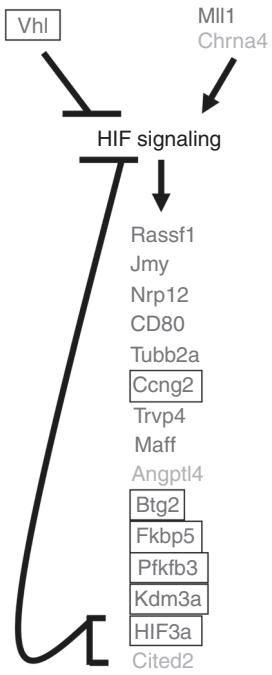


**Fig. 3** Genes differentially expressed in the RNAseq data (false discovery rate < 0.1 in ≥2 differential expression tools) in hypoxia-inducible factor (HIF) signaling. Upregulated, downregulated, or no change. Boxes indicate genes selected for quantitative PCR in a validation cohort, along with HIF-1α and HIF-2α

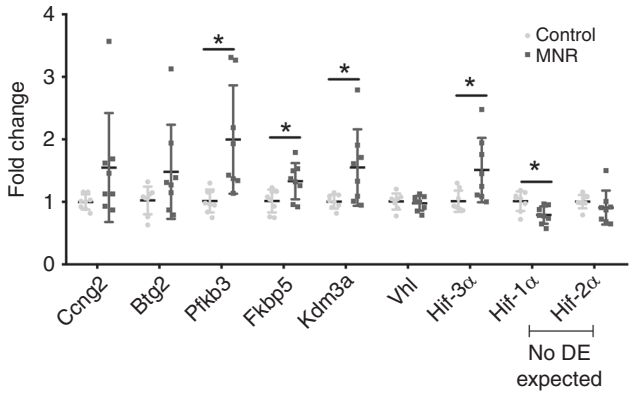


**Fig. 4** Relative fold change for genes involved in hypoxia-inducible factor signaling validated in an additional cohort with qPCR. Data are plotted as mean ± SEM and asterisks represent $p < 0.05$ with an unpaired *t* test. Control $N = 8$ and maternal nutrient restriction $N = 8$, 1 or 2 pups/litter

it to stabilize and accumulate longer than HIF-1a.[24,25] In addition, differential expression of miRNAs can lead to decreased Hif-1a mRNA stability but not Hif-2a.[26] HIF-1a and HIF-2a have both redundant and non-redundant gene targets that depend on cellular context and cell type.[27] The presence of HIF-2a but not HIF-1a is likely due to the late-gestational sampling in this study and duration of hypoxia signaling.

After formation of the liver bud (~E10), hepatoblasts begin to differentiate into biliary cells and then immature hepatocytes.[28] When fetal livers were collected in this study (E18.5),

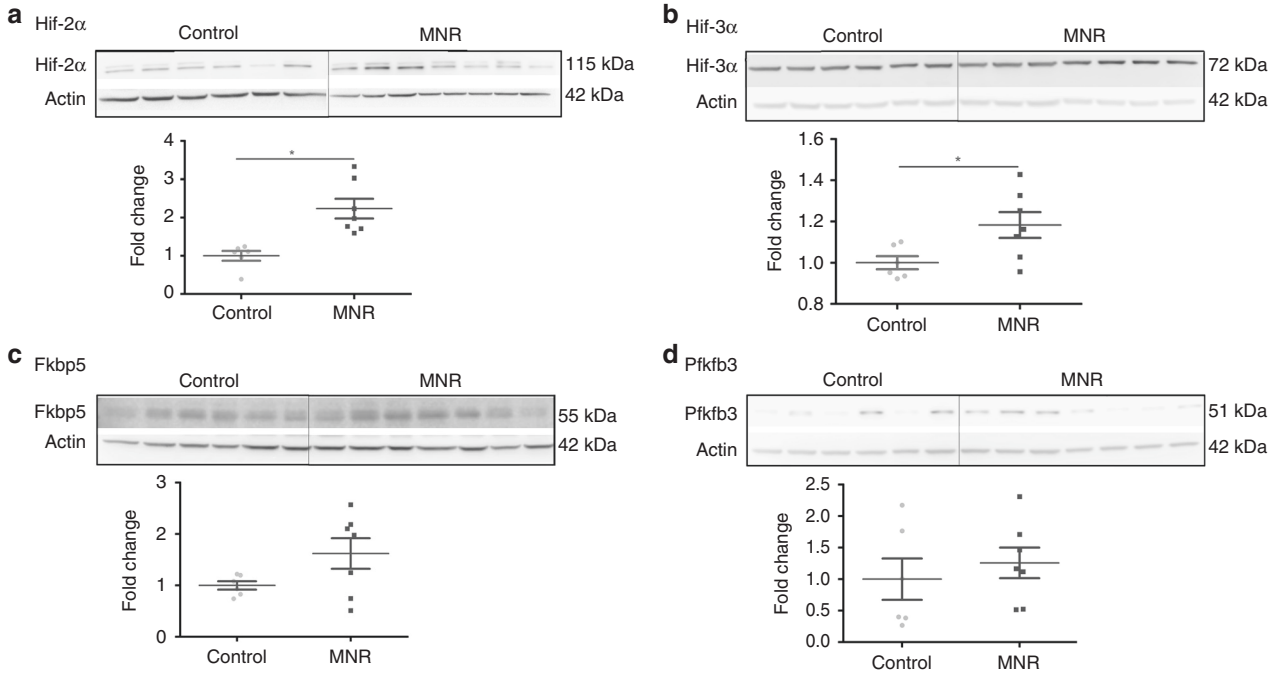


**Fig. 5** Western blots of proteins confirmed to be differentially expressed in the validation cohort. Hypoxia-inducible factor (HIF)-2α (**a**) and HIF-3α (**b**) were significantly increased in maternal nutrient restriction (MNR) offspring by 2.2- and 1.3-fold ($p = 0.002$ and 0.03, respectively). FKBP5 (**c**) and PFKFB3 (**d**) were not significantly different in MNR relative to controls ($p = 0.09$ and 0.5, respectively). All blots were run in triplicates and representative blots are shown. Data are plotted as mean ± SEM and asterisks represent $p < 0.05$ with an unpaired *t* test. Control $N = 6$ and MNR $N = 7$, 1 or 2 pups/litter

differentiation into hepatocytes and hepatic outgrowth would be occurring and would continue into the perinatal period.[28] Studies in human induced embryonic stem cell liver buds and in the livers from fetal mice suggest that HIF-1a expression is positively associated with differentiation into biliary cells and negatively correlated with differentiation into hepatocytes.[29] Conversely, HIF-2a regulates proliferation and hepatic outgrowth in zebra fish.[30] Given the distinct roles, disruption in the timing or protein level of HIFs could alter liver development. Models of MNR, including ours,[11] have demonstrated reduced liver size (Radford and Han, 2018),[11] reduced transcription of genes promoting proliferation, and increased transcription of markers for differentiation.[31] While further studies to characterize temporal changes of HIF signaling induced by MNR are needed, increased hepatic HIF signaling late in gestation could indicate altered timing of differentiation and proliferation during liver development.

Hif-3a mRNA and protein were higher in MNR compared to controls. Hif-3a mRNA is induced by HIF-1a during chronic hypoxia and transcriptionally downregulates Hif-1a as a negative feedback mechanism.[32,33] In mice, Hif-3a has three isoforms, a full-length transcript and two variants, IPAS and NPAS. All three isoforms can inhibit the transcriptional activity of HIFs by binding with HIF-1β or HIF-1/2a, preventing dimerization and nuclear translocation.[34] Some HIF-3a splice variants can also weakly induce canonical HIF-1a target genes.[35] Consequently, increased HIF-3a protein could contribute to moderate differences between control and MNR HIF-induced transcription.

Fkbp5 was also increased at the transcript level and, although not significant, relatively increased at the protein level. FK506-binding protein (FKBP5) is induced by chronic hypoxia in adipose tissue[36] and the induction is HIF-2a dependant in hepatocellular carcinoma cell lines.[37] It functions as co-chaperon to HSP90 and as a scaffold protein. Subsequently, FKBP5 has diverse functions, including reducing glucocorticoid receptor activity[38] and promoting adipocyte differentiation[36] and AKT dephosphorylation.[39] Other studies have been conducted in cancer cell lines or adipocytes, but the role in the developing liver in unknown. It is conceivable that increased FKBP5 transcription could be an attempt to adjust metabolism and/or cell growth but that is not sufficient to induce changes at the protein level due to post-translational regulation. Posttranslational regulation of HIF target genes such as FKBP5 could also play a role in the maladaptive response to MNR in the developing liver.

Changes to hypoxia signaling in the liver could be indirect through placental adaptations. In guinea pigs, MNR results in increased hypoxyprobe-1 staining in both male and female liver and kidneys.[8] However, no differences were detected in the placentas.[8] Alternatively, MNR causes fetal circulation to distribute oxygenated blood received from the umbilical cord away from the liver to the brain.[40] MNR could increase HIF signaling in the developing liver through changes to fetal circulation and/or nutritional signaling. Further studies into the mechanism of HIF signaling need to be elucidated. However, increased HIF-induced transcripts support the concept that MNR results in increased hypoxia signaling in the fetal liver.

MNR resulted in fetal expression changes in hypoxia-inducible signaling pathways of E18.5 liver. Although expression changes were detected, the protein levels of genes induced by HIF transcription factors were not significantly different. Since tissue hypoxia declines during development,[21,29] it is possible that downstream changes were more evident earlier in liver development. Still, owing to their importance in regulating multipotency, cell differentiation, and proliferation, HIF-induced transcription could result in differences in liver maturity and cell populations. In addition, differential expression of epigenetic regulators such as KDM3a may prime HRE-containing genes to respond differentially to aging or nutritional abundance. Evidence of aberrant hypoxia signaling was evident in growth-restricted mice, but the impact was moderate that may relate to the duration of nutrient restriction and the timing of analysis. Differentially expressed transcripts support the concept that hypoxia signaling may play a role in growth restriction in response to fetal undernutrition.

## ACKNOWLEDGEMENTS

Guidance in bioinformatic analysis was provided by Dr. Greg Gloor. Library preparation and sequencing was completed at McGill University and Genome Quebec Innovation Centre, Quebec, Canada. Grant support for these studies were provided by the Canadian Institutes of Health Research (to V.K.M.H.), Douglas and Vivian Bocking Chair in Fetal and Newborn Growth from St. Joseph's Health Care Foundation (to V.K.M.H. and B.N.R.), and the Children's Health Foundation (to V.K.M.H.).

## AUTHOR CONTRIBUTIONS

Experimental design, collection and analysis of data, and drafting of the manuscript was done by B.N.R. V.K.M.H. provided guidance in experimental design, revised the manuscript, and provided study funding.

## ADDITIONAL INFORMATION

The online version of this article (https://doi.org/10.1038/s41390-019-0447-z) contains supplementary material, which is available to authorized users.

**Competing interests:** The authors declare no competing interests.

**Publisher's note:** Springer Nature remains neutral with regard to jurisdictional claims in published maps and institutional affiliations.

## REFERENCES

1. Han, V. K. M., Seferovic, M. D., Albion, C. D. & Gupta, M. B. in *Neonatology* (eds Buonocore, G., Bracci, R. & Weindling, M.) 89–93 (Springer, Milano, 2012).
2. Hales, C. N. & Barker, D. J. P. Type 2 (non-insulin-dependent) diabetes mellitus: the thrifty phenotype hypothesis. *Int. J. Epidemiol.* **42**, 1215–1222 (2013).
3. Oliveira, D. et al. Protein restriction during the last third of pregnancy malprograms the neuroendocrine axes to induce metabolic syndrome in adult male rat offspring. *Endocrinology* **157**, 1799–1812 (2016).
4. Bruick, R. K. & McKnight, S. L. A conserved family of prolyl-4-hydroxylases that modify HIF. *Science* **294**, 1337–1340 (2001).
5. Brahimi-Horn, C., Mazure, N. & Pouysségur, J. Signalling via the hypoxia-inducible factor-1α requires multiple posttranslational modifications. *Cell. Signal.* **17**, 1–9 (2005).
6. Slemc, L. & Kunej, T. Transcription factor HIF1A: downstream targets, associated pathways, polymorphic hypoxia response element (HRE) sites, and initiative for standardization of reporting in scientific literature. *Tumour Biol.* **37**, 14851–14861 (2016).
7. Paauw, N. D. et al. H3K27 acetylation and gene expression analysis reveals differences in placental chromatin activity in fetal growth restriction. *Clin. Epigenet.* **10**, 85 (2018).
8. Elias, A. A. et al. Maternal nutrient restriction in guinea pigs leads to fetal growth restriction with evidence for chronic hypoxia. *Pediatr. Res* **82**, 141–147 (2017).
9. Rajakumar, A. et al. Placental HIF-1 alpha, HIF-2 alpha, membrane and soluble VEGF receptor-1 proteins are not increased in normotensive pregnancies complicated by late-onset intrauterine growth restriction. *Am. J. Physiol. Regul. Integr. Comp. Physiol.* **293**, R766–R774 (2007).
10. Lewis, R. M., James, L. A., Zhang, J., Byrne, C. D. & Hales, C. N. Effects of maternal iron restriction in the rat on hypoxia-induced gene expression and fetal metabolite levels. *Br. J. Nutr.* **85**, 193–201 (2001).
11. Radford, B. N. & Han, V. K. M. Offspring from maternal nutrient restriction in mice show variations in adult glucose metabolism similar to human fetal growth 3 restriction. *J. Dev. Orig. Health Dis.* https://doi.org/10.1017/S2040174418000983 (2018).
12. Lecoutre, S. et al. Maternal undernutrition programs the apelinergic system of adipose tissue in adult male rat offspring. *J. Dev. Orig. Health Dis.* https://doi.org/10.1017/S2040174416000702 (2017).
13. Karolchik, D. et al. The UCSC Table Browser data retrieval tool. *Nucleic Acids Res.* **32**, D493–D496 (2004).
14. Langmead, B. & Salzberg, S. L. Fast gapped-read alignment with Bowtie 2. *Nat. Methods* **9**, 357–359 (2012).
15. Edgar, R., Domrachev, M. & Lash, A. E. Gene Expression Omnibus: NCBI gene expression and hybridization array data repository. *Nucleic Acids Res.* **30**, 207–210 (2002).
16. Robinson, M. D., McCarthy, D. J. & Smyth, G. K. edgeR: a Bioconductor package for differential expression analysis of digital gene expression data. *Bioinformatics* **26**, 139–140 (2010).
17. Love, M. I., Huber, W. & Anders, S. Moderated estimation of fold change and dispersion for RNA-seq data with DESeq2. *Genome Biol.* **15**, 550 (2014).
18. Fernandes, A. D., Macklaim, J. M., Linn, T. G., Reid, G. & Gloor, G. B. ANOVA-like differential expression (ALDEx) analysis for mixed population RNA-Seq. *PLoS ONE* **8**, e67019 (2013).
19. Mi, H. et al. PANTHER version 11: expanded annotation data from Gene Ontology and Reactome pathways, and data analysis tool enhancements. *Nucleic Acids Res.* **45**, D183–D189 (2017).
20. Kuleshov, M. V. et al. Enrichr: a comprehensive gene set enrichment analysis web server 2016 update. *Nucleic Acids Res.* **44**, W90–W97 (2016).
21. Koh, M. Y. & Powis, G. Passing the baton: the HIF switch. *Trends Biochem. Sci.* **37**, 364–372 (2012).
22. Serocki, M. et al. miRNAs regulate the HIF switch during hypoxia: a novel therapeutic target. *Angiogenesis* **21**, 183–202 (2018).
23. Holmquist-Mengelbier, L. et al. Recruitment of HIF-1alpha and HIF-2alpha to common target genes is differentially regulated in neuroblastoma: HIF-2alpha promotes an aggressive phenotype. *Cancer Cell* **10**, 413–423 (2006).
24. Berra, E. et al. HIF prolyl-hydroxylase 2 is the key oxygen sensor setting low steady-state levels of HIF-1α in normoxia. *EMBO J.* **22**, 4082–4090 (2003).
25. Bracken, C. P. et al. Cell-specific regulation of hypoxia-inducible factor (HIF)-1alpha and HIF-2alpha stabilization and transactivation in a graded oxygen environment. *J. Biol. Chem.* **281**, 22575–22585 (2006).
26. Bruning, U. et al. MicroRNA-155 promotes resolution of hypoxia-inducible factor 1alpha activity during prolonged hypoxia. *Mol. Cell Biol.* **31**, 4087–4096 (2011).
27. Hu, C.-J., Wang, L.-Y., Chodosh, L. A., Keith, B. & Simon, M. C. Differential roles of hypoxia-inducible factor 1alpha (HIF-1alpha) and HIF-2alpha in hypoxic gene regulation. *Mol. Cell Biol.* **23**, 9361–9374 (2003).
28. Si-Tayeb, K., Lemaigre, F. P. & Duncan, S. A. Organogenesis and development of the liver. *Dev. Cell* **18**, 175–189 (2010).
29. Ayabe, H. et al. Optimal hypoxia regulates human iPSC-derived liver bud differentiation through intercellular TGFB signaling. *Stem Cell Rep.* **11**, 306–316 (2018).
30. Lin, T.-Y. et al. Hypoxia-inducible factor 2 alpha is essential for hepatic outgrowth and functions via the regulation of leg1 transcription in the zebrafish embryo. *PLoS ONE* **9**, e101980 (2014).
31. Boylan, J. M., Sanders, J. A. & Gruppuso, P. A. Regulation of fetal liver growth in a model of diet restriction in the pregnant rat. *Am. J. Physiol. Regul. Integr. Comp. Physiol.* **311**, R478–R488 (2016).
32. Tanaka, T., Wiesener, M., Bernhardt, W., Eckardt, K.-U. & Warnecke, C. The human HIF (hypoxia-inducible factor)-3alpha gene is a HIF-1 target gene and may modulate hypoxic gene induction. *Biochem. J.* **424**, 143–151 (2009).
33. Ravenna, L. et al. Distinct phenotypes of human prostate cancer cells associate with different adaptation to hypoxia and pro-inflammatory gene expression. *PLoS ONE* **9**, e96250 (2014).
34. Ravenna, L., Salvatori, L. & Russo, M. A. HIF3α: the little we know. *FEBS J.* **283**, 993–1003 (2016).
35. Zhang, P. et al. Hypoxia-inducible factor 3 is an oxygen-dependent transcription activator and regulates a distinct transcriptional response to hypoxia. *Cell Rep.* **6**, 1110–1121 (2014).
36. Zhang, L. et al. Loss of FKBP5 impedes adipocyte differentiation under both normoxia and hypoxic stress. *Biochem. Biophys. Res. Commun.* **485**, 761–767 (2017).
37. Xu, J. et al. Increasing AR by HIF-2 inhibitor (PT-2385) overcomes the side-effects of sorafenib by suppressing hepatocellular carcinoma invasion via alteration of pSTAT3, pAKT and pERK signals. *Cell Death Dis.* **8**, e3095 (2017).
38. Antunica-Noguerol, M. et al. The activity of the glucocorticoid receptor is regulated by SUMO conjugation to FKBP51. *Cell Death Differ.* **23**, 1579–1591 (2016).
39. Luo, K. et al. USP49 negatively regulates tumorigenesis and chemoresistance through FKBP51-AKT signaling. *EMBO J.* **36**, 1434–1446 (2017).
40. López-Tello, J. et al. Characterization of early changes in fetoplacental hemodynamics in a diet-induced rabbit model of IUGR. *J. Dev. Orig. Health Dis.* **6**, 454–461 (2015).